Published in final edited form as:
Vet Microbiol. 2010 February 24; 141(1-2): 12. doi:10.1016/j.vetmic.2009.07.035.

Equine herpesvirus type 1 (EHV-1) utilizes microtubules, dynein, and ROCK1 to productively infect cells.

Arthur R. Frampton Jr.[1,*,†], **Hiroaki Uchida**[1], **Jens von Einem**[2], **William F. Goins**[1], **Paola Grandi**[3], **Justus B. Cohen**[1], **Nikolaus Osterrieder**[2,4], and **Joseph C. Glorioso**[1]

[1]Department of Microbiology and Molecular Genetics, University of Pittsburgh, School of Medicine, Pittsburgh, PA 15261

[2]Department of Microbiology and Immunology, College of Veterinary Medicine, Cornell University, Ithaca, NY 14853

[3]Department of Neurological Surgery, University of Pittsburgh, School of Medicine, Pittsburgh, PA, 15261

[4]Institut für Virologie, Freie Universität Berlin, 10115 Berlin Germany

Abstract

To initiate infection, equine herpesvirus type 1 (EHV-1) attaches to heparan sulfate on cell surfaces and then interacts with a putative glycoprotein D receptor(s). After attachment, virus entry occurs either by direct fusion of the virus envelope with the plasma membrane or via endocytosis followed by fusion between the virus envelope and an endosomal membrane. Upon fusion, de-enveloped virus particles are deposited into the cytoplasm and travel to the nucleus for viral replication. In this report, we examined the mechanism of EHV-1 intracellular trafficking and investigated the ability of EHV-1 to utilize specific cellular components to efficiently travel to the nucleus post-entry. Using a panel of microtubule depolymerizing drugs and inhibitors of microtubule motor proteins, we show that EHV-1 infection is dependent on both the integrity of the microtubule network and the minus-end microtubule motor protein, dynein. In addition, we show that EHV-1 actively induces the acetylation of tubulin, a marker of microtubule stabilization, as early as 15 minutes post-infection. Finally, our data support a role for the cellular kinase, ROCK1, in virus trafficking to the nucleus.

Keywords

EHV-1; trafficking; microtubules; dynein; ROCK1

1. Introduction

Equine herpesvirus 1 (EHV-1) is a major pathogen of horses. Most horses are exposed to the virus within 6 months to a year after birth and are frequently re-infected throughout their lifetime (Allen, 1986). Clinical signs that appear early after infection include fever,

*To whom correspondence should be addressed.
†Current affiliation: Arthur R. Frampton Jr. Ph.D Assistant Professor University of North Carolina Wilmington Department of Biology and Marine Biology Phone: (910) 962-2643 Fax: (910)962-4066 framptona@uncw.edu

inappattence, malaise, coughing, and mucopurulent discharge (O'Callaghan et al., 1983). As the infection progresses, horses may exhibit signs of serious neurological illness including ataxia, disorientation, and partial to full paralysis. In addition to the neurological sequelae, EHV-1 also causes abortigenic disease in pregnant mares.

At the cellular level, EHV-1 must engage host cellular proteins and induce specific signaling pathways very early in infection in order to successfully infect cells. EHV-1 initially binds to target cells via an interaction between viral glycoproteins B and C and glycosaminoglycans on the plasma membrane (Sugahara et al., 1997, Osterrieder, 1999). After attachment, a putative entry receptor is recognized (Frampton et al., 2005) by glycoprotein D (Csellner et al., 2000). The next step in the EHV-1 entry pathway varies depending upon the cell type (Frampton et al., 2007). EHV-1 fuses with the plasma membrane and deposits de-enveloped particles into the cytoplasm of equine dermal (ED) and rabbit kidney (RK-13) cells. On the contrary, fully enveloped particles are endocytosed in CHO-K1 cells and naked capsids are then released into the cytosol after the virus fuses with the endosomal membrane. Regardless of the initial mode of entry, we recently showed that the cellular kinase Rho associated coiled-coil kinase 1 (ROCK1) must be induced for the virus to complete the infection process (Frampton et al., 2007).

Once inside the cells, EHV-1 must traverse the intricate meshwork of the intracellular cytoskeleton in order to reach the nucleus and deposit the viral genome. The mechanisms employed by EHV-1 to traffic to the nucleus have yet to be defined, but certain clues are provided by studies with other viruses that utilize microtubules and their associated machinery for intracellular trafficking. Microtubules are composed of α and β dimers of tubulin and contain a structural polarity with a positive end that is oriented toward the periphery of the cell and a negative end that is anchored at the microtubule organizing center (MTOC) adjacent to the nucleus (Nogales, 2000). To reach the nucleus, many viruses attach themselves to, and are directionally propelled by dynein, a minus-end directed microtubule motor, towards the MTOC (Kelkar et al., 2004, Alonso et al., 2001, Suikkanen et al., 2003, Petit et al., 2003, Ye et al., 2000, Douglas et al., 2004, Jacob et al., 2000, Raux et al., 2000, Florin et al., 2006). Sodeik et al. initially showed that the alphaherpesvirus herpes simplex virus type 1 (HSV-1) uses microtubules to traffic to the nucleus. Their data revealed that nuclear transport of HSV-1 was significantly inhibited in the presence of the microtubule-depolymerizing drugs, nocodazole, vinblastine, or colchicine (Sodeik et al., 1997). The movement of HSV-1 capsids along microtubules was also shown to require dynein as expression of the dynein inhibitor, dynamitin (Dohner et al., 2002), and specific inhibitors of dynein ATPase (Lee et al., 2006, Kobayashi et al., 1978, Kristensson et al., 1986, Penningroth et al., 1982) decreased HSV-1 transport to the nucleus. The movement of virus particles was also shown to be independent of microtubule turnover or treadmilling (microtubule polymerization/depolymerization) as the microtubule-stabilizing drug paclitaxel had no effect on nucleocapsid transport (Sodeik et al., 1997).

In addition to utilizing microtubules for transport, viruses also generate an intracellular environment that is conducive for nuclear transport by triggering various signaling pathways. One common theme is the induction of signaling pathways that lead to the reorganization of cytoskeletal components. Many viruses, including HSV-1, stimulate members of the Ras GTPase superfamily and this induction can lead to a wide array of morphological changes of infected cells, including, but not limited to, stabilization of microtubules (Naranatt et al., 2005), formation of focal adhesions (Cheshenko et al., 2005) and endocytosis or phagocytosis (Clement et al., 2006).

In this study, we show that EHV-1 causes the stabilization of microtubules via the acetylation of tubulin and utilizes the minus-end directed microtubule motor dynein to traffic to the nucleus

along stabilized microtubules. In addition, we show that nuclear accumulation of capsids is decreased in the presence of the ROCK1 inhibitor, Y-27632.

2. Materials and methods

2.1. Cells, viruses, and plasmids

RK-13 cells were grown in Dulbecco's modified Eagle medium (DMEM) supplemented with 10% fetal bovine serum (FBS) (Invitrogen, Carlsbad, CA). Chinese hamster ovary (CHO-K1) cells were kindly provided by Dr. Patricia Spear (Northwestern University, Chicago, IL) and grown in F12-K media (Invitrogen) supplemented with 10% FBS. Equine dermal cells (ED), a gift from Dr. Ron Montelaro (University of Pittsburgh, Pittsburgh, PA), were maintained in minimal essential medium (MEM) supplemented with 10% FBS. All cells were maintained at 37°C in 5% CO_2.

The EHV-1 recombinant virus L11ΔgIΔgE contains a *lacZ* reporter cassette in place of gI and gE (Frampton et al., 2002). The EHV-1 recombinant virus L11VP26mRed was described previously (J. von Einem et al., 24th annual ASV meeting 2005). This recombinant virus contains an mRFP1 fluorescent protein fused to the EHV-1 VP26 small capsid protein.

2.2. Drug inhibition assays

For entry assays, 2.5×10^4 ED or CHO-K1 cells were seeded in a 96-well plate. The next day, cells were incubated with increasing amounts of the microtubule depolymerizing drugs, nocodazole, vinblastine, colchicine, the microtubule stabilizing drug, paclitaxel (PTX), the dynein inhibitor, EHNA (erythro-9-(2-hydroxy-3-nonyl) adenine, or the kinesin inhibitor AMP-PNP (adenosine 5′-(β, γ-imido) triphosphate tetralithium salt) (Sigma, St. Louis, MO) at 37°C for 30 min. Cells were infected with EHV-1 (L11ΔgIΔgE) at an MOI of 5 and incubated for 5.5 h in the presence of the drugs at 37°C. Cells were washed once with PBS and then ONPG was added to the cells and the absorbance read at 405nm. Triplicate samples were measured for each concentration of drug. A 1mM stock of paclitaxel was prepared in distilled H_2O. One-hundred mM stock solutions of EHNA and nocodazole were prepared in DMSO. A 100 mM stock solution of AMP-PNP was prepared in H_2O. 10 mM stocks of the ROCK1 inhibitor, Y-27632 (EMD Biosciences, La Jolla, CA) were made in H_2O. 10mM stocks of vinblastine, and colchicine were also made in H_2O. Cell viability was measured in triplicate using the CellTiter 96 aqueous non-radioactive cell proliferation assay (Promega, Madison, WI) following the manufacturer's protocol.

2.3. Western Blot Analyses

Confluent ED cells in a 12-well plate were serum starved for 1 h and cells were then mock-treated or treated with paclitaxel (10 μM) or Y-27632 (100 μM). Cells treated with paclitaxel were washed with MEM at 15, 30, and 60 min and cell lysates were harvested with PARP lysis buffer (6 M urea, 2% SDS, 10% glycerol, 62.5 mM Tris-HCl, pH 6.8, and 5% β-mercaptoethanol). Mock-treated cells or cells treated with Y-27632 were infected with EHV-1 (L11VP26mRed) at an MOI of 10 in the presence or absence of Y-27632. At 15, 30, and 60 min post-infection, cells were washed once with MEM and lysates were harvested with PARP lysis buffer. Samples were run on a 10% SDS-PAGE gel and transferred to an immobilon-P membrane (Millipore, Billerica, MA). The membranes were blocked for 1 h in 10% non-fat dry milk (NFDM) at room temperature (RT) before monoclonal anti-acetylated tubulin antibody 6-11B-1 (Sigma) was added at a concentration of 1:2000 in TBST with 5% NFDM for 16 h at 4°C. The membranes were washed 3x for 10 min/wash and then anti-mouse-HRP antibody SC-2031 (Santa Cruz Biotechnology, Santa Cruz, CA) was added at a concentration of 1:3,000 in TBST with 5% NFDM for 1 h at RT. Membranes were washed 3x for 10 min/wash then ECL detection reagent (Amersham Biosciences, Buckinghamshire, England) was

added and the membranes exposed to film. After stripping the membrane with stripping buffer (10% SDS, 0.5M Tris pH 6.8, 0.5% β-mercaptoethanol) for 30 min at 50°C, the membranes were washed 2x for 10 min/wash with TBST and then blocked for 1 h with 10% NFDM. Total tubulin was detected by adding monoclonal anti-α-tubulin antibody B-5-1-2 (Sigma) at 1:2,000 for 16 h at 4°C with the secondary antibody and detection steps as described earlier.

2.4. Infectious virus recovery assay

4×10^5 cells in 24-well plates were incubated with 100 μM of Y-27632 in DMEM or DMEM alone for 30 min at 37°C. Plates were placed on ice for 5 min and then EHV-1 (MOI = 10) in DMEM or DMEM containing 100 μM Y-27632 was incubated on the cells at 4°C for 3 h. Cells were washed once with cold DMEM and then warm media (37°C) was added to the cells. At each time-point, cells were washed with glycine (pH 3.0) for 30 s, washed once with DMEM, and harvested. Virus samples were freeze-thawed once then sonicated 3x for 15 s. Virus harvested from each time-point was titered on RK13 cells. Triplicate samples were measured for each time-point.

2.5. Confocal microscopy of EHV-1 infected cells

CHO-K1 cells were seeded to confluency in collagen-coated 35 mm dishes (MatTek Corporation, Ashland, MA). Cells were mock-treated or treated with 100 μM Y-27632 or 10 μM paclitaxel for 30 min at 37°C. Cells were chilled on ice for 10 min and then L11VP26mRed was added to the cells at an MOI of 10. Virus was incubated on the cells at 4°C for 2 h in the presence or absence of drug. After 2 h, cells for the 0 time-point were fixed with 4% paraformaldehyde (PFA) at 4°C. Media pre-warmed to 37°C, with or without drug, was added to the remaining cells and then the cells were fixed with 4% PFA at 15, 30, 60, and 120 min post temperature shift. After 30 min of fixation with 4% PFA, cells were rehydrated with PBS for 15 min at 4°C. Cells were washed once more with PBS for 15 min and then cells were examined using an inverted Olympus Fluo-View 1000 confocal microscope (Olympus America Inc., Center Valley, PA). Prior to imaging, cells were stained with Hoechst dye (1 μg/mL) and wheat germ agglutinin (5 μg/mL) to label the nucleus and plasma membrane, respectively. All images were captured at a 60x magnification.

3. Results

3.1. EHV-1 utilizes microtubules for infection

To determine if EHV-1 requires microtubules for infection, a virus entry assay was performed in the presence or absence of microtubule depolymerizing agents. Equine dermal (ED) cells were untreated or treated with increasing concentrations of nocodazole, vinblastine, or colchicine for 30 min prior to infection and the drugs were kept on the cells throughout the experiment. Cells were infected with L11ΔgIΔgE, an EHV-1 recombinant virus containing a *lacZ* reporter gene, at an MOI of 5 for 5.5 hours. EHV-1 infection, as measured by β-galactosidase expression, was significantly inhibited in a dose-dependent manner by all of the drugs. Nocodazole inhibited infection by 80% at the highest concentration tested (Figure 1A) and vinblastine (Figure 1B) and colchicine (Figure 1C) inhibited infection by 82% and 56%, respectively. This inhibition of infection was not the result of drug-associated cell toxicity as cell viability was similar for all of the concentrations used. In addition to inhibiting infection on ED cells, these drugs also inhibited infection on CHO-K1 cells (data not shown). These results indicate that an intact microtubule network is required regardless of the mode of EHV-1 entry.

To address the importance of microtubule dynamics or treadmilling (polymerization/depolymerization of microtubules) in virus transport, microtubules were first stabilized with paclitaxel or left untreated before and during infection with EHV-1. Virus entry was assessed

by measuring β-galactosidase activity 5.5 h post-infection. In both ED (Fig 2A) and CHO-K1 (Fig 2B) cells, stabilization of microtubules prior to the addition of EHV-1 had no effect on infection as measured by viral reporter gene expression. To assure that paclitaxel treatment of ED cells induced microtubule stabilization, we examined the acetylation of tubulin, which has been shown to be a reliable indicator of stable or fixed microtubules (Piperno et al., 1987). Western blotting was performed to detect acetylated tubulin at 15, 30, and 60 minutes post-treatment with 10 μM paclitaxel. As shown in Figure 3, paclitaxel treatment resulted in the hyperacetylation of tubulin as early as 15 minutes post-treatment and the level of acetylation steadily increased the longer the cells were treated with the drug.

The ability of EHV-1 to travel to the nucleus after microtubule stabilization was assessed by infecting CHO-K1 cells with the fluorescently tagged-EHV-1 recombinant L11VP26mRed in the presence or absence of paclitaxel. This recombinant virus contains a red fluorescent protein fused to the VP26 capsid protein and thus the subcellular localization of this virus can be detected throughout a time course of infection by confocal microscopy. CHO-K1 cells were untreated or treated with 10 μM of paclitaxel for 30 minutes and then virus was added and allowed to attach to the cells at 4°C for 2 hours to synchronize the entry process. After attachment, medium warmed to 37°C, with or without addition of the drug, was added to the cells to allow infection to ensue. At 0 and 60 minutes post-temperature shift, cells were stained with Hoechst dye and wheat germ agglutinin to label the nucleus (blue) and plasma membrane (green), respectively. As shown in Figure 4, attached virus (red) was detected on the surface of mock-treated and paclitaxel-treated cells at the 0 time-point. At the 60-minute time-point, a similar number of capsids were observed at the nucleus in both mock-treated and paclitaxel-treated cells. The ability of virus to reach the nucleus after paclitaxel stabilization of microtubules in a manner similar to that observed in mock-treated cells suggests that EHV-1 is efficiently transported along stable microtubules and that there is not a requirement for a continuous process of microtubule polymerization/depolymerization (treadmilling) for successful delivery of EHV-1 to the nucleus.

3.2. EHV-1 infection induces the acetylation of tubulin

The ability of EHV-1 to traffic along stable microtubules led us to ask whether EHV-1 actively induces the stabilization of microtubules. To test this possibility, we compared the amount of acetylated tubulin between mock and EHV-1 infected cells by western blot assay. Other viruses, including HSV-1 (Elliott and O'Hare, 1998), KSHV (Naranatt et al., 2005, Raghu et al., 2007) and African Swine Fever Virus (Jouvenet et al., 2004) have been shown to induce the acetylation of tubulin upon infection and in some cases this event has been linked to the activity of Rho-signaling proteins (Naranatt et al., 2005, Raghu et al., 2007). Since ROCK1 is a proximal effector of Rho signaling, we also tested whether the inhibition of ROCK1 would have any effect on the ability of EHV-1 to induce the acetylation of tubulin. ED cells were untreated or treated with the ROCK1 inhibitor Y-27632 for 30 min and then either mock-infected or infected with EHV-1 at an MOI of 10 for 15, 30, and 60 minutes. As shown in Figure 5, EHV-1 infection resulted in a significant induction of acetylated tubulin as early as 15 minutes post-infection and the amount of acetylated tubulin increased over time. The ROCK1 inhibitor had no effect on the ability of EHV-1 to cause the acetylation of tubulin. These results indicate that EHV-1 actively induces the acetylation of microtubules and that this process is not dependent upon the activation of ROCK1.

3.3. The microtubule motor, dynein, is essential for EHV-1 infection

Dynein is a minus-end directed motor that transports intracellular cargo along microtubules and many intracellular pathogens, including HSV (Sodeik et al., 1997), have been shown to utilize dynein for transport to the nucleus. To determine if EHV-1 needs dynein for efficient transport to the nucleus and thus infection, we utilized the dynein inhibitor, EHNA, which

blocks the ability of dynein to hydrolyze ATP (Ravikumar et al., 2005, Penningroth et al., 1982, Bouchard et al., 1981, Dhani et al., 2003, Cheung et al., 2004). ED cells were infected with L11ΔgIΔgE in the presence or absence of EHNA and β-galactosidase expression was measured as an indicator of virus infection (Fig. 6A). As a control, cells were treated with AMP-PNP, which inhibits the plus-end directed motor, kinesin. Infection was significantly reduced in cells treated with EHNA, but not in cells treated with AMP-PNP. At the highest concentration of EHNA tested (1 mM), infection was inhibited by 68%. Neither drug was toxic to the cells at the concentrations used as measured by an MTS cell viability assay. The inhibition of EHV-1 infection by EHNA indicates that EHV-1 utilizes dynein for movement to the nucleus post-entry.

Since the initial entry process of EHV-1 in CHO-K1 cells is different from entry into ED cells, we asked whether dynein was also employed for intracellular movement of EHV-1 in CHO-K1 cells. Entry of EHV-1 into CHO-K1 cells was also inhibited by EHNA in a dose-dependent manner (Fig 6B). These data suggest that, while the initial entry of EHV-1 into different cell types is dissimilar, the virus uses the same molecular machinery for transport post-entry.

3.4. Inhibition of ROCK1 deregulates the intracellular processing of EHV-1

In a previous study, we showed that the activation of ROCK1 is critical for productive EHV-1 infection (Frampton et al., 2007). One possible step that ROCK1 might be required for in the EHV-1 life cycle is at the initial stage of virus uptake into cells. To test this possibility, we performed an infectious virus recovery assay on CHO-K1 cells in the presence or absence of the ROCK1 inhibitor, Y-27632. This assay allows for the recovery of fully enveloped virus particles from endosomal vesicles at different time points post-infection. CHO-K1 cells were untreated or treated with Y-27632 for 30 min at 37°C (Fig. 7). Cells were then chilled to 4°C and EHV-1 was added with or without drug and allowed to attach to cells for 3 hours at 4°C. After virus attachment, the temperature was raised to 37°C and virus was incubated on cells for up to 3 hours in the presence or absence of Y-27632. At the indicated times post-temperature shift, extracellular virus was inactivated by washing the cells with an acidic buffer, and intracellular virus was harvested and titered as described in materials and methods. No difference was observed in the amount of infectious virus recovered at 15 minutes, indicating that ROCK1 did not exert an effect on initial EHV-1 uptake into cells. However, there was a significant spike in the amount of virus recovered at the 30-minute time-point in the presence of Y-27632. After the 30-minute time point the amount of virus recovered from untreated and Y-27632 cells was virtually the same. The increased recovery of virus at 30 minutes in the presence of the ROCK1 inhibitor suggests that ROCK1 mediates its effect at a time post virus entry.

3.5. Decreased nuclear localization of EHV-1 in the presence of the ROCK1 inhibitor, Y-27632

To examine if ROCK1 inhibition disrupts EHV-1 trafficking, CHO-K1 cells were infected with the fluorescent EHV-1 recombinant virus L11VP26mRed in the presence or absence of the ROCK1 inhibitor, Y-27632 (Fig. 8). Cells were untreated (Fig. 8A) or treated with Y-27632 (Fig. 8B) for 30 minutes at 37°C and then virus was added and allowed to attach to cells for 2 hours at 4°C. After the attachment period, cells were warmed to 37°C to allow for virus entry. Infected cells were fixed and imaged at 0 to 120 minutes post-temperature shift using a confocal microscope. At the 0 time-point, virus particles were attached to the plasma membrane (yellow circles) and no particles were observed inside either the untreated or Y-27632-treated cells. At 15 minutes post-infection, internal and external virus particles were observed in both groups. Interestingly, as shown in Figure 8A about one-third of the virus particles were localized to the nucleus in the mock-treated cells (white circles) at 15 minutes post-infection, but only two virus particles were observed at the nucleus in the Y-27632-treated cells (Fig. 8B). Over the course of infection, more virus particles accumulated at the nucleus in the untreated cells (Fig.

8A) compared to the cells treated with Y-27632 (Fig. 8B) and the majority of particles in the Y-27632-treated cells remained associated with the plasma membrane. These data show that treatment of cells with Y-27632 significantly inhibits the movement of EHV-1 to the nucleus and indicate that ROCK1 is critical for the intracellular trafficking of EHV-1.

4. Discussion

Many viruses exploit the cellular machinery to travel intracellularly. One common theme that has emerged as an integral part of the lifecycle of viruses is the co-opting of cellular motors, which are normally used to traffic various cargoes throughout the cell. Upon entry into cells, many viruses bind to molecular motors that are tethered to microtubules [for review see (Dohner et al., 2005)]. Microtubules are dynamic structures that act as cellular tracks, which viruses utilize to move directionally toward the nucleus of the cell where replication ensues. After replication and assembly, viruses utilize another set of cellular motors for egress. Without the use of these cellular motors for transport, viruses would never be able to find their way through the dense and intricate cytoskeletal structures and would thus fail to replicate and release progeny virus.

In this study, we show that EHV-1 utilizes the microtubule network and the minus-end directed motor protein dynein to productively infect cells. Disruption of the microtubular network with the microtubule depolymerizing agents nocodazole, vinblastine, and colchicine inhibited the ability of EHV-1 to productively infect cells and deliver its payload to the nucleus. In addition, the introduction of dynein, but not kinesin inhibitors, also reduced infection. Interestingly, microtubules and dynein were required for virus trafficking in cells that were infected via an endocytic route or by direct fusion of virus at the plasma membrane. These data suggest at least two possible models for intracellular trafficking of EHV-1 particles that we have designated as the direct and the indirect trafficking model. In the direct model, nucleocapsids that are still surrounded by some tegument proteins would bind to dynein via a viral capsid or tegument protein and this event would therefore occur only after completion of the fusion event between the viral envelope and either the plasma or endosomal membrane. In the indirect model, EHV-1 would be transported within an endosome and an endosomal protein or complex would interact with dynein. Virus would then fuse and be released from the endosome once it is in close proximity to the nucleus. The ability of EHV-1 to enter some cells by direct fusion at the cell membrane implies that a direct interaction between a viral protein and a dynein component most likely has to occur for the virus to traffic to the nucleus. However, since EHV-1 enters other cell types via an endocytic mechanism, it is possible that the indirect model of trafficking applies in these cells and thus the mechanism of intracellular movement of virus toward the nucleus may be cell-type dependent. Studies are currently underway using L11VP26mRed in conjunction with dynein and endosomal marker antibodies to further explore these models.

An intriguing finding from this study is the importance of the Rho kinase, ROCK1, for intracellular trafficking of EHV-1 particles. Previously, we showed that inhibition of this kinase significantly reduced EHV-1 infection (Frampton et al., 2007), but we did not address the mechanism. In the current study, we showed that treatment with a ROCK1 inhibitor significantly decreased the number of capsids that accumulated at the nucleus suggesting a role for ROCK1 in the intracellular trafficking of EHV-1.

While this is the first report to connect ROCK1 activation with virus trafficking, previous studies have shown that other molecules involved in the ROCK1 signaling pathway also contribute to virus movement within cells. Naranatt and colleagues reported that inactivation of the RhoA GTPase, which acts directly upstream of ROCK1, blocks the delivery of KSHV to the nucleus (Naranatt et al., 2005). In addition, their data support a model in which virus binding to cells activates RhoA, which in turn leads to microtubule stabilization via acetylation

and an increased ability of the virus to traffic towards the nucleus (Raghu et al., 2007). This microtubule stabilization was further shown to occur after induction of Dia-2 (Naranatt et al., 2005) a member of the diaphanous-related formin family involved in cytoskeletal rearrangements and a downstream effector of RhoA. Consistent with these reports, other groups have shown that many viruses including adenoviruses and the *alphaherpesvirus*, HSV-1, travel along stabilized microtubules. Sodeik et al. showed that stabilization of microtubules with paclitaxel prior to HSV-1 infection had no effect on the nuclear accumulation of capsids (Sodeik et al., 1997) and Mabit et al. showed that paclitaxel treatment slightly increased nuclear delivery of capsids (Mabit et al., 2002). These studies revealed that microtubule dynamics, or treadmilling, are not required for HSV-1 capsid trafficking. The finding in our current study that EHV-1 infection actively induces the stabilization of microtubules and that infection is not negatively affected by the prior stabilization of microtubules suggests a common mechanism of microtubule transport of nucleocapsids that is shared amongst alphaherpesviruses.

The connection between EHV-1-induced microtubule stabilization, virus trafficking along stabilized microtubules, and the dependence of virus trafficking on ROCK1 function would suggest a direct role for the RhoA-ROCK1 signaling pathway in microtubule stabilization. However, one group showed that while RhoA is required for this effect, it is not mediated through ROCK1 (Palazzo et al., 2001). Consistent with these data, our results revealed that the inhibition of EHV-1 infection by Y-27632 did not inhibit EHV-1-induced stabilization of microtubules. We therefore concluded that the contribution of ROCK1 to virus trafficking is most likely separate from virus-induced microtubule stabilization.

The observation that many virus particles remain associated with the plasma membrane in the presence of the ROCK1 inhibitor Y-27632 suggests other possible roles for ROCK1 in virus trafficking. Two intriguing possibilities are that 1) ROCK1 activity is required in order to mediate an interaction between virus and microtubules and/or other cytoskeletal components or 2) ROCK1 is required for efficient fusion of the viral envelope with a cellular membrane. Inhibition of either of these processes could account for the inability of EHV-1 to traffic to the nucleus. Future studies will examine which virus components are involved in the initiation of signaling pathways that lead to both ROCK1 activation and separately the acetylation of microtubules.

5. Conclusion

In the current study we examined some of the early interactions between EHV-1 and host cell factors and, in particular, investigated how EHV-1 utilizes the cell's microtubular network and associated proteins to efficiently infect susceptible cells. Our results showed that disruption of microtubules by the addition of microtubule-depolymerizing agents and the inhibition of the microtubule motor protein, dynein, significantly abrogated EHV-1 infection in ED and CHO-K1 cells. Our data also revealed that stabilization of microtubules by paclitaxel prior to infection had no impact on the efficiency of EHV-1 infection in either cell type. Interestingly, our data showed that microtubules are acetylated very early after infection with EHV-1. Whether this acetylation is an absolute requirement for EHV-1 infection is an intriguing question and efforts are underway to address this possibility. Finally, we showed that inhibition of the cellular kinase ROCK1 with the drug Y-27632, inhibited the movement of EHV-1 capsids to the nucleus. These ROCK1 data follow-up on our earlier study, showing that ROCK1 activation is critical for EHV-1 infection (Frampton et al., 2007). Future studies will aim to define how ROCK1 is activated by EHV-1, what specific cellular events are reliant upon this activation, and how these cellular events contribute to a productive infection. Knowledge obtained from these studies may be translated into the development of antiviral compounds

that can be used to inhibit the identified critical processes that EHV-1 needs to complete its pathogenic program within the horse.

Acknowledgments

We thank Patricia Spear for providing the CHO cell lines and Ron Montelaro for the ED cells. We thank Simon Watkins for the use of the confocal microscope. This work was supported by NIH grants CA119298, NS44323, NS040923, and HL066949.

References

ALLEN GP, BRYANS JT. Molecular epizootiology, pathogenesis, and prophylaxis of equine herpesvirus-1 infections. Prog. Vet. Microbiol. Immunol 1986;2:78–144. [PubMed: 2856183]

ALONSO C, MISKIN J, HERNAEZ B, FERNANDEZ-ZAPATERO P, SOTO L, CANTO C, RODRIGUEZ-CRESPO I, DIXON L, ESCRIBANO JM. African swine fever virus protein p54 interacts with the microtubular motor complex through direct binding to light-chain dynein. J Virol 2001;75:9819–27. [PubMed: 11559815]

BOUCHARD P, PENNINGROTH SM, CHEUNG A, GAGNON C, BARDIN CW. erythro-9-[3-(2-Hydroxynonyl)]adenine is an inhibitor of sperm motility that blocks dynein ATPase and protein carboxylmethylase activities. Proc Natl Acad Sci U S A 1981;78:1033–6. [PubMed: 6453342]

CHESHENKO N, LIU W, SATLIN LM, HEROLD BC. Focal adhesion kinase plays a pivotal role in herpes simplex virus entry. J Biol Chem 2005;280:31116–25. [PubMed: 15994312]

CHEUNG PY, ZHANG Y, LONG J, LIN S, ZHANG M, JIANG Y, WU Z. p150(Glued), Dynein, and microtubules are specifically required for activation of MKK3/6 and p38 MAPKs. J Biol Chem 2004;279:45308–11. [PubMed: 15375157]

CLEMENT C, TIWARI V, SCANLAN PM, VALYI-NAGY T, YUE BY, SHUKLA D. A novel role for phagocytosis-like uptake in herpes simplex virus entry. J Cell Biol 2006;174:1009–21. [PubMed: 17000878]

CSELLNER H, WALKER C, WELLINGTON JE, MCLURE LE, LOVE DN, WHALLEY JM. EHV-1 glycoprotein D (EHV-1 gD) is required for virus entry and cell-cell fusion, and an EHV-1 gD deletion mutant induces a protective immune response in mice. Arch Virol 2000;145:2371–85. [PubMed: 11205124]

DHANI SU, MOHAMMAD-PANAH R, AHMED N, ACKERLEY C, RAMJEESINGH M, BEAR CE. Evidence for a functional interaction between the ClC-2 chloride channel and the retrograde motor dynein complex. J Biol Chem 2003;278:16262–70. [PubMed: 12601004]

DOHNER K, NAGEL CH, SODEIK B. Viral stop-and-go along microtubules: taking a ride with dynein and kinesins. Trends Microbiol 2005;13:320–7. [PubMed: 15950476]

DOHNER K, WOLFSTEIN A, PRANK U, ECHEVERRI C, DUJARDIN D, VALLEE R, SODEIK B. Function of dynein and dynactin in herpes simplex virus capsid transport. Mol Biol Cell 2002;13:2795–809. [PubMed: 12181347]

DOUGLAS MW, DIEFENBACH RJ, HOMA FL, MIRANDA-SAKSENA M, RIXON FJ, VITTONE V, BYTH K, CUNNINGHAM AL. Herpes simplex virus type 1 capsid protein VP26 interacts with dynein light chains RP3 and Tctex1 and plays a role in retrograde cellular transport. J Biol Chem 2004;279:28522–30. [PubMed: 15117959]

ELLIOTT G, O'HARE P. Herpes simplex virus type 1 tegument protein VP22 induces the stabilization and hyperacetylation of microtubules. J Virol 1998;72:6448–55. [PubMed: 9658087]

FLORIN L, BECKER KA, LAMBERT C, NOWAK T, SAPP C, STRAND D, STREECK RE, SAPP M. Identification of a dynein interacting domain in the papillomavirus minor capsid protein l2. J Virol 2006;80:6691–6. [PubMed: 16775357]

FRAMPTON AR JR. GOINS WF, COHEN JB, VON EINEM J, OSTERRIEDER N, O'CALLAGHAN DJ, GLORIOSO JC. Equine herpesvirus 1 utilizes a novel herpesvirus entry receptor. J Virol 2005;79:3169–73. [PubMed: 15709036]

FRAMPTON AR JR. SMITH PM, ZHANG Y, MATSUMURA T, OSTERRIEDER N, O'CALLAGHAN DJ. Contribution of gene products encoded within the unique short segment of equine herpesvirus 1 to virulence in a murine model. Virus Res 2002;90:287–301. [PubMed: 12457983]

FRAMPTON AR JR. STOLZ DB, UCHIDA H, GOINS WF, COHEN JB, GLORIOSO JC. Equine Herpesvirus 1 Enters Cells by Two Different Pathways, and Infection Requires the Activation of the Cellular Kinase ROCK1. J Virol 2007;81:10879–89. [PubMed: 17670830]

JACOB Y, BADRANE H, CECCALDI PE, TORDO N. Cytoplasmic dynein LC8 interacts with lyssavirus phosphoprotein. J Virol 2000;74:10217–22. [PubMed: 11024152]

JOUVENET N, MONAGHAN P, WAY M, WILEMAN T. Transport of African swine fever virus from assembly sites to the plasma membrane is dependent on microtubules and conventional kinesin. J Virol 2004;78:7990–8001. [PubMed: 15254171]

KELKAR SA, PFISTER KK, CRYSTAL RG, LEOPOLD PL. Cytoplasmic dynein mediates adenovirus binding to microtubules. J Virol 2004;78:10122–32. [PubMed: 15331745]

KOBAYASHI T, MARTENSEN T, NATH J, FLAVIN M. Inhibition of dynein ATPase by vanadate, and its possible use as a probe for the role of dynein in cytoplasmic motility. Biochem Biophys Res Commun 1978;81:1313–8. [PubMed: 149544]

KRISTENSSON K, LYCKE E, ROYTTA M, SVENNERHOLM B, VAHLNE A. Neuritic transport of herpes simplex virus in rat sensory neurons in vitro. Effects of substances interacting with microtubular function and axonal flow [nocodazole, taxol and erythro-9-3-(2-hydroxynonyl) adenine]. J Gen Virol 1986;67(Pt 9):2023–8. [PubMed: 2427647]

LEE GE, MURRAY JW, WOLKOFF AW, WILSON DW. Reconstitution of herpes simplex virus microtubule-dependent trafficking in vitro. J Virol 2006;80:4264–75. [PubMed: 16611885]

MABIT H, NAKANO MY, PRANK U, SAAM B, DOHNER K, SODEIK B, GREBER UF. Intact microtubules support adenovirus and herpes simplex virus infections. J Virol 2002;76:9962–71. [PubMed: 12208972]

NARANATT PP, KRISHNAN HH, SMITH MS, CHANDRAN B. Kaposi's sarcoma-associated herpesvirus modulates microtubule dynamics via RhoA-GTP-diaphanous 2 signaling and utilizes the dynein motors to deliver its DNA to the nucleus. J Virol 2005;79:1191–206. [PubMed: 15613346]

NOGALES E. Structural insights into microtubule function. Annu Rev Biochem 2000;69:277–302. [PubMed: 10966460]

O'CALLAGHAN, DJ.; GENTRY, GA.; RANDALL, CC. The equine herpesviruses. In: ROIZMAN, B., editor. The Herpesviruses, Comprehensive Virology. Plenum Press; New York: 1983.

OSTERRIEDER N. Construction and characterization of an equine herpesvirus 1 glycoprotein C negative mutant. Virus Res 1999;59:165–77. [PubMed: 10082388]

PALAZZO AF, COOK TA, ALBERTS AS, GUNDERSEN GG. mDia mediates Rho-regulated formation and orientation of stable microtubules. Nat Cell Biol 2001;3:723–9. [PubMed: 11483957]

PENNINGROTH SM, CHEUNG A, BOUCHARD P, GAGNON C, BARDIN CW. Dynein ATPase is inhibited selectively in vitro by erythro-9-[3-2-(hydroxynonyl)]adenine. Biochem Biophys Res Commun 1982;104:234–40. [PubMed: 6462140]

PETIT C, GIRON ML, TOBALY-TAPIERO J, BITTOUN P, REAL E, JACOB Y, TORDO N, DE THE H, SAIB A. Targeting of incoming retroviral Gag to the centrosome involves a direct interaction with the dynein light chain 8. J Cell Sci 2003;116:3433–42. [PubMed: 12857789]

PIPERNO G, LEDIZET M, CHANG XJ. Microtubules containing acetylated alpha-tubulin in mammalian cells in culture. J Cell Biol 1987;104:289–302. [PubMed: 2879846]

RAGHU H, SHARMA-WALIA N, VEETTIL MV, SADAGOPAN S, CABALLERO A, SIVAKUMAR R, VARGA L, BOTTERO V, CHANDRAN B. Lipid rafts of primary endothelial cells are essential for Kaposi's sarcoma-associated herpesvirus/human herpesvirus 8-induced phosphatidylinositol 3-kinase and RhoA-GTPases critical for microtubule dynamics and nuclear delivery of viral DNA but dispensable for binding and entry. J Virol 2007;81:7941–59. [PubMed: 17507466]

RAUX H, FLAMAND A, BLONDEL D. Interaction of the rabies virus P protein with the LC8 dynein light chain. J Virol 2000;74:10212–6. [PubMed: 11024151]

RAVIKUMAR B, ACEVEDO-AROZENA A, IMARISIO S, BERGER Z, VACHER C, O'KANE CJ, BROWN SD, RUBINSZTEIN DC. Dynein mutations impair autophagic clearance of aggregate-prone proteins. Nat Genet 2005;37:771–6. [PubMed: 15980862]

SODEIK B, EBERSOLD MW, HELENIUS A. Microtubule-mediated transport of incoming herpes simplex virus 1 capsids to the nucleus. J Cell Biol 1997;136:1007–21. [PubMed: 9060466]

SUGAHARA Y, MATSUMURA T, KONO Y, HONDA E, KIDA H, OKAZAKI K. Adaptation of equine herpesvirus 1 to unnatural host led to mutation of the gC resulting in increased susceptibility of the virus to heparin. Arch Virol 1997;142:1849–56. [PubMed: 9672642]

SUIKKANEN S, AALTONEN T, NEVALAINEN M, VALILEHTO O, LINDHOLM L, VUENTO M, VIHINEN-RANTA M. Exploitation of microtubule cytoskeleton and dynein during parvoviral traffic toward the nucleus. J Virol 2003;77:10270–9. [PubMed: 12970411]

YE GJ, VAUGHAN KT, VALLEE RB, ROIZMAN B. The herpes simplex virus 1 U(L)34 protein interacts with a cytoplasmic dynein intermediate chain and targets nuclear membrane. J Virol 2000;74:1355–63. [PubMed: 10627546]

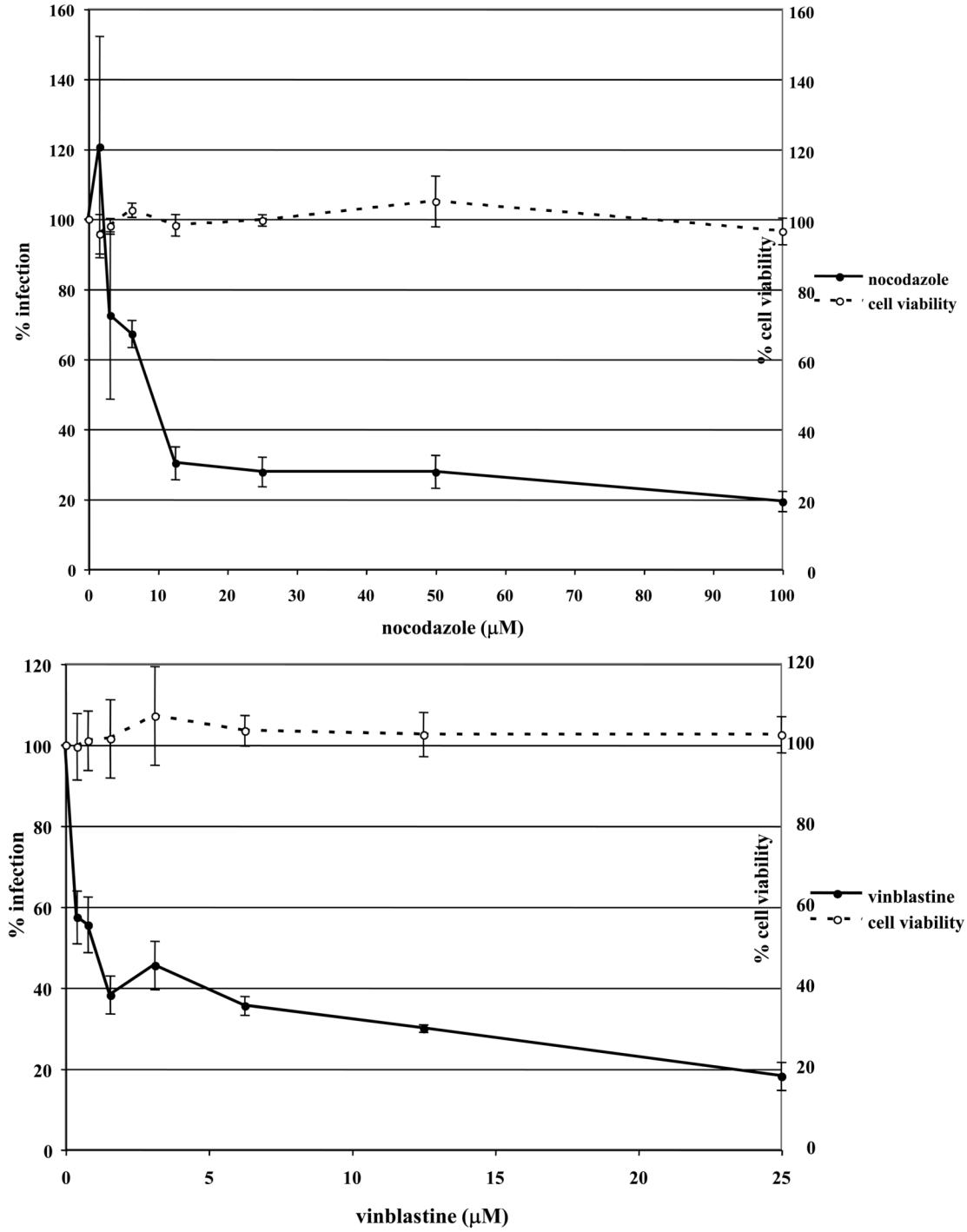

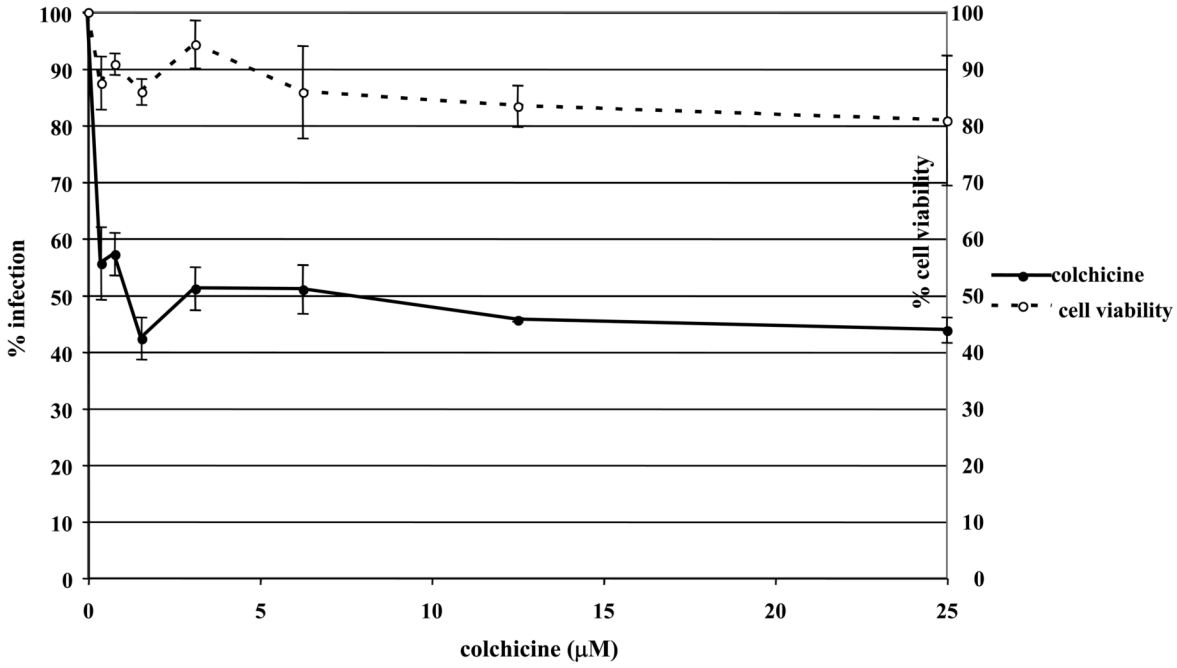

Fig. 1.

Depolymerization of microtubules inhibits EHV-1 infection. Triplicate cultures of ED cells were mock-treated or treated with increasing amounts of the microtubule depolymerizing drugs (A) nocodazole, (B) vinblastine, or (C) colchicine for 30 min at 37°C and then infected with EHV-1 (L11ΔgIΔgE) at an MOI of 5 for 5.5 h in the presence of the drugs. β-galactosidase expression was measured by an ONPG assay (filled circles). Absorbance at 405nm was measured for each sample and A_{405nm} values from infected cells that were not treated with drug were set as 100% infection. Cell viability at each concentration of drug was measured by an MTS assay (open circles) and viability of cells that were not treated with drug was set at 100%.

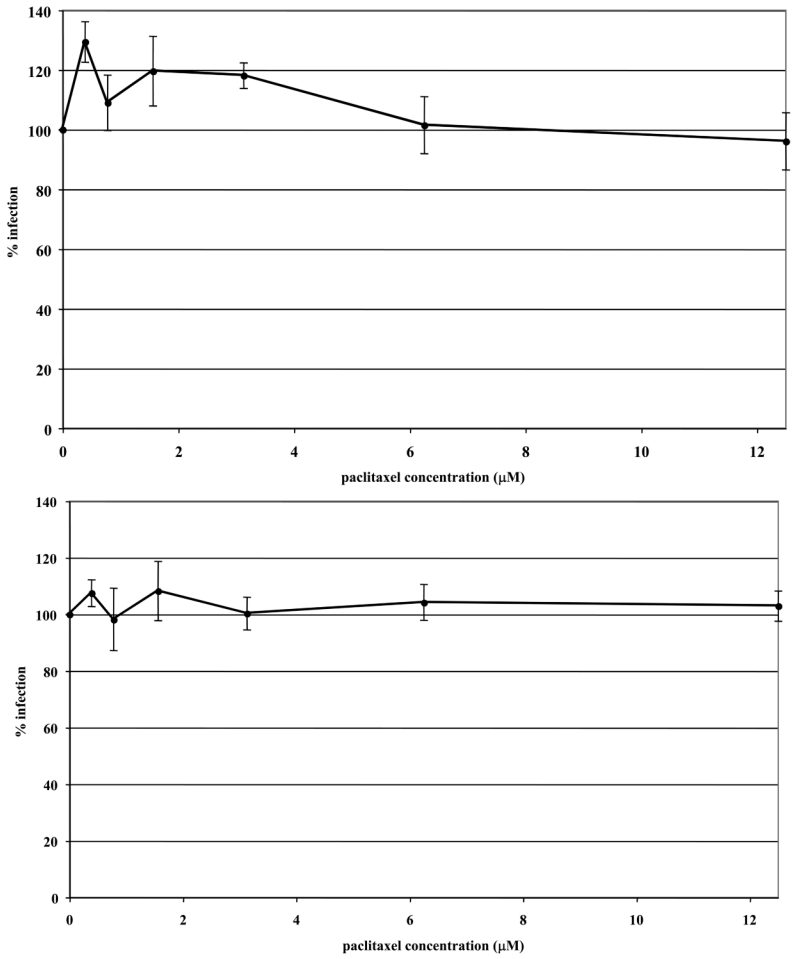

Fig. 2.

Stabilization of microtubules does not inhibit EHV-1 infection. Triplicate cultures of ED (A) or CHO-K1 (B) cells were mock-treated or treated with increasing amounts of the microtubule-stabilizing compound, paclitaxel (PTX) for 30 min at 37°C and then infected with EHV-1 (L11ΔgIΔgE) at an MOI of 5 for 5.5 h in the presence of the drug. β-galactosidase expression was measured by an ONPG assay (filled circles). Absorbance at 405nm was measured for each sample and A_{405nm} values from infected cells that were not treated with drug were set as 100% infection.

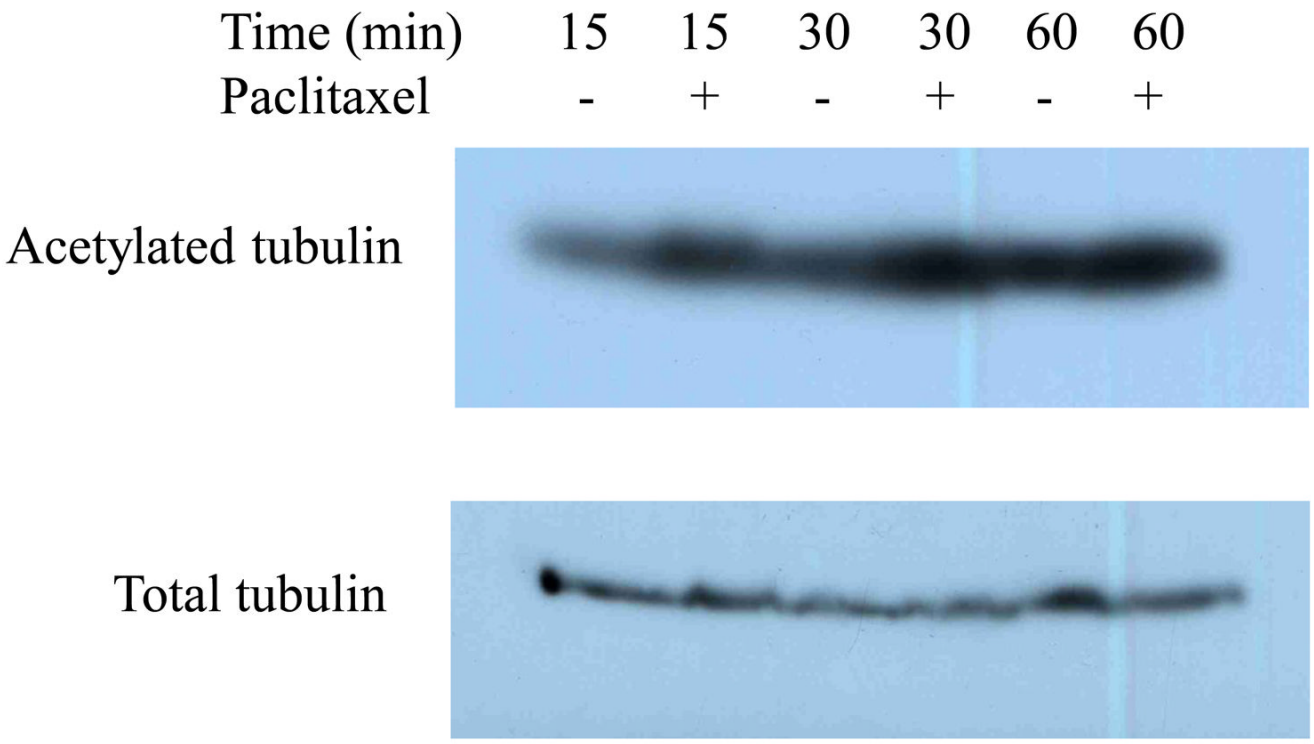

Fig. 3.
Paclitaxel (PTX) stabilization of microtubules. ED cells were serum-starved for 1 h and then mock-treated or treated with 10 μM of paclitaxel for 15, 30, or 60 min. Acetylated and total tubulin were detected by western blot as described in Materials and Methods.

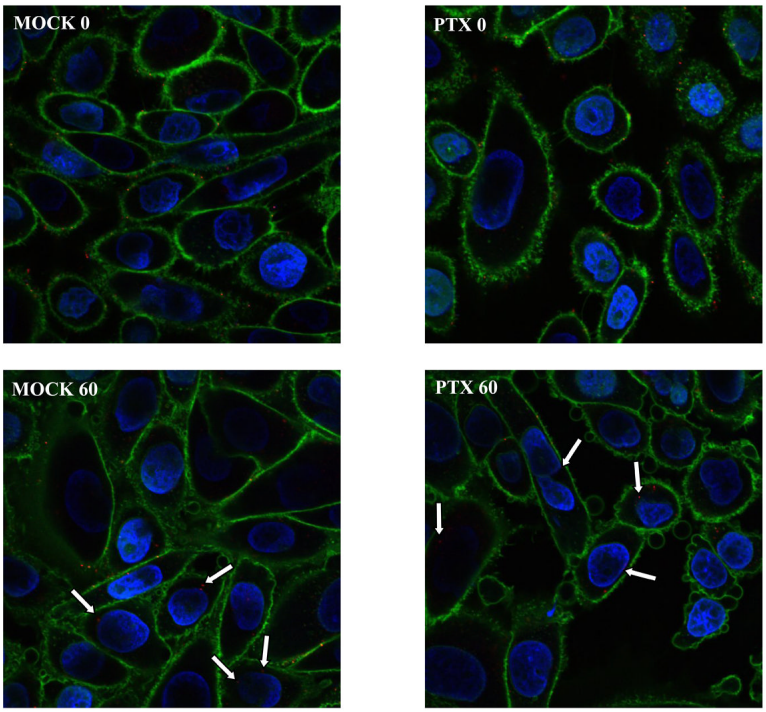

Fig. 4.

Paclitaxel (PTX) treatment of cells has no effect on EHV-1 infection. CHO-K1 cells were mock treated or treated with 10 μM of PTX for 30 min at 37°C. Cells were chilled on ice for 10 min and then L11VP26mRed was incubated on the cells at 4°C for 2 h in the presence or absence of PTX (10μM). 37°C media with or without PTX was added to the cells and then the cells were fixed and stained at 0 and 60 min with Hoechst and wheat germ agglutinin to label the nucleus (blue) and plasma membrane (green), respectively. Capsids (red) were observed with a confocal microscope. White arrows indicate peri-nuclear capsids.

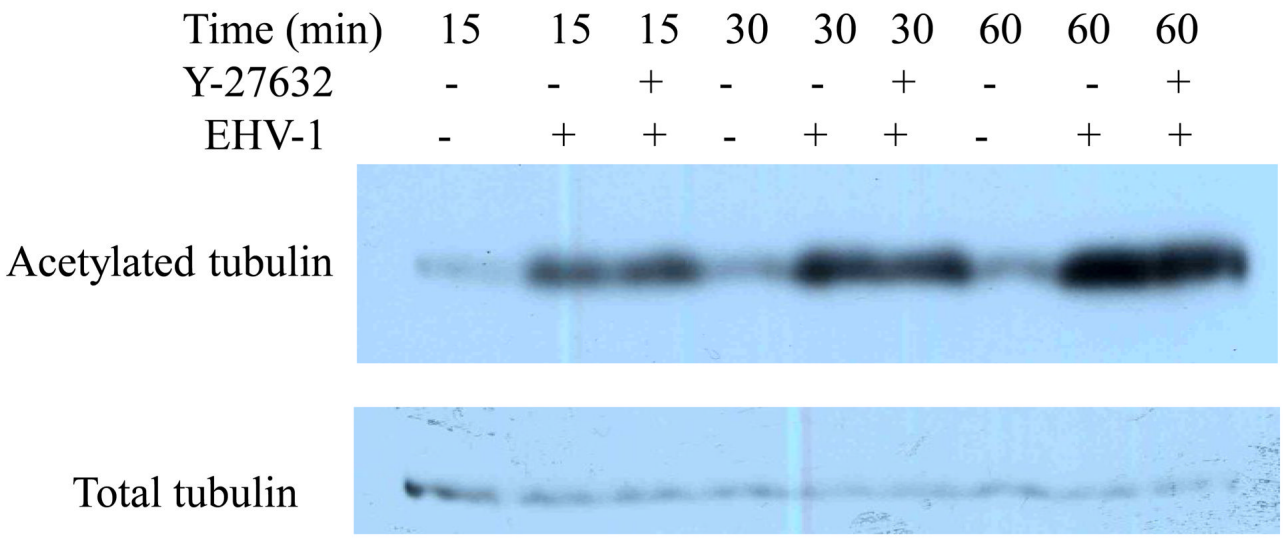

Fig. 5.

EHV-1 induces the acetylation of tubulin. ED cells were serum starved for 1 h and then mock-treated or treated with Y-27632 for 30 min. Cells were mock-infected or infected with EHV-1 (L11VP26mRed) at an MOI of 10 in the presence or absence of Y-27632. Acetylated and total tubulin were detected by western blot at 15, 30, and 60 min post-infection as described in Materials and Methods.

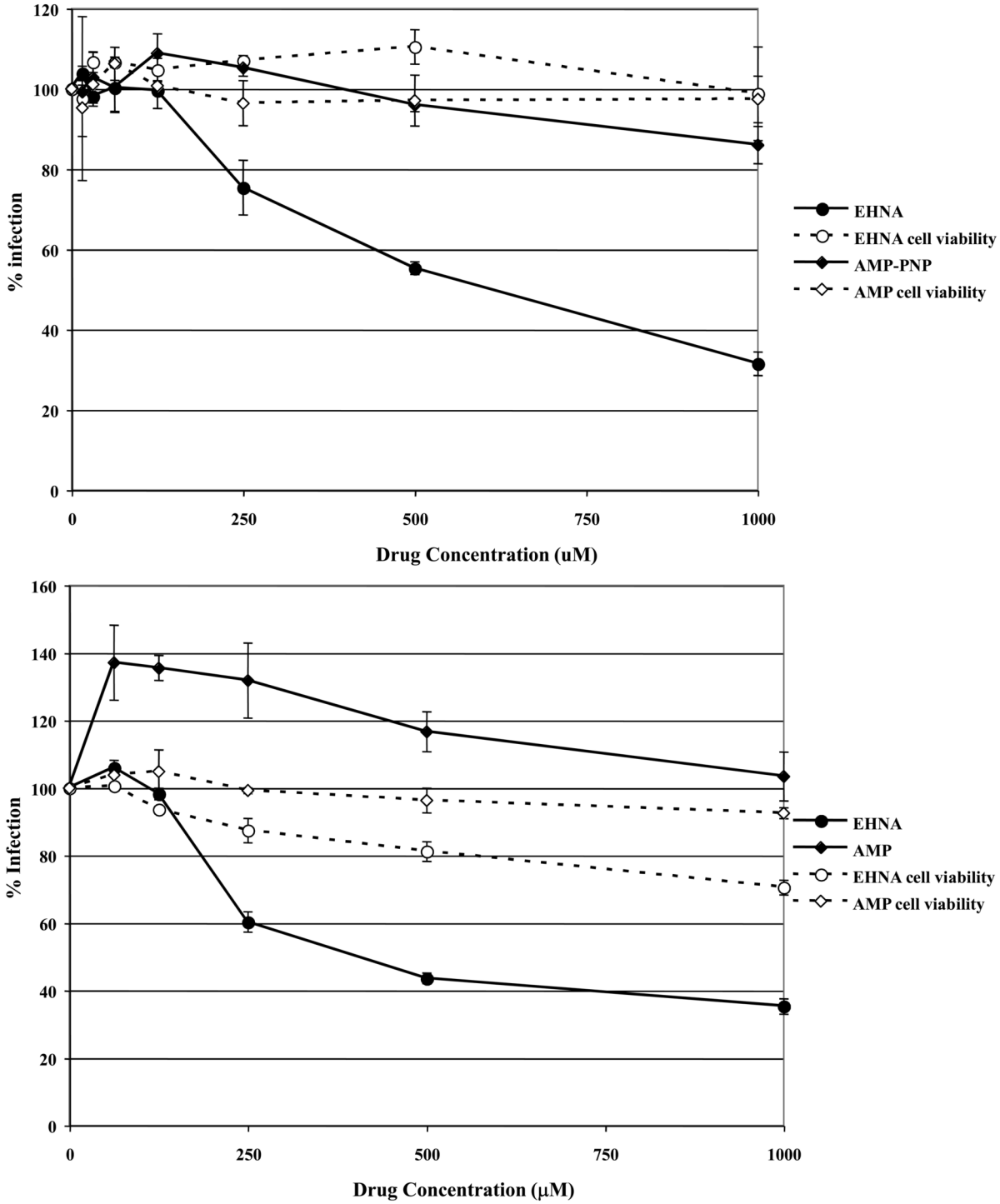

Fig. 6.

Inhibition of dynein with EHNA blocks EHV-1 infection. Triplicate cultures of (A) ED or (B) CHO-K1 cells were mock-treated or treated with increasing amounts of EHNA (filled circles) or AMP-PNP (filled diamonds) for 30 min at 37°C and then infected with EHV-1 (L11ΔgIΔgE) at an MOI of 5 for 5.5 h in the presence of the drugs. β-galactosidase expression

was measured by ONPG assay and cell viability at each concentration of drug was measured by MTS assay, EHNA (open circles), AMP-PNP (open diamonds).

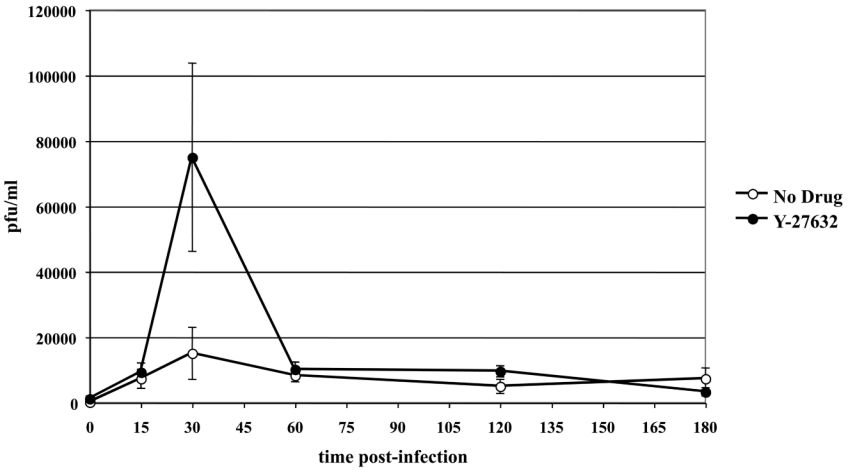

Fig. 7.

Increased infectious EHV-1 recovery in the presence of the ROCK inhibitor, Y-27632. Triplicate cultures of CHO-K1 cells were either mock-treated (open circles) or treated with 100 μM of Y-27632 (closed circles) for 30 min at 37°C. Cells were chilled on ice for 10 min and then L11ΔgIΔgE at an MOI of 10 was bound to the cells at 4°C for 2h in the presence or absence of Y-27632. Cells were washed and cold media was replaced with 37°C media. At the indicated times, cells were treated with an acidic buffer (pH 3.0) to inactivate non-internalized virus and the cells were washed with media. Internalized virus was harvested from cells and titered on RK13 cells.

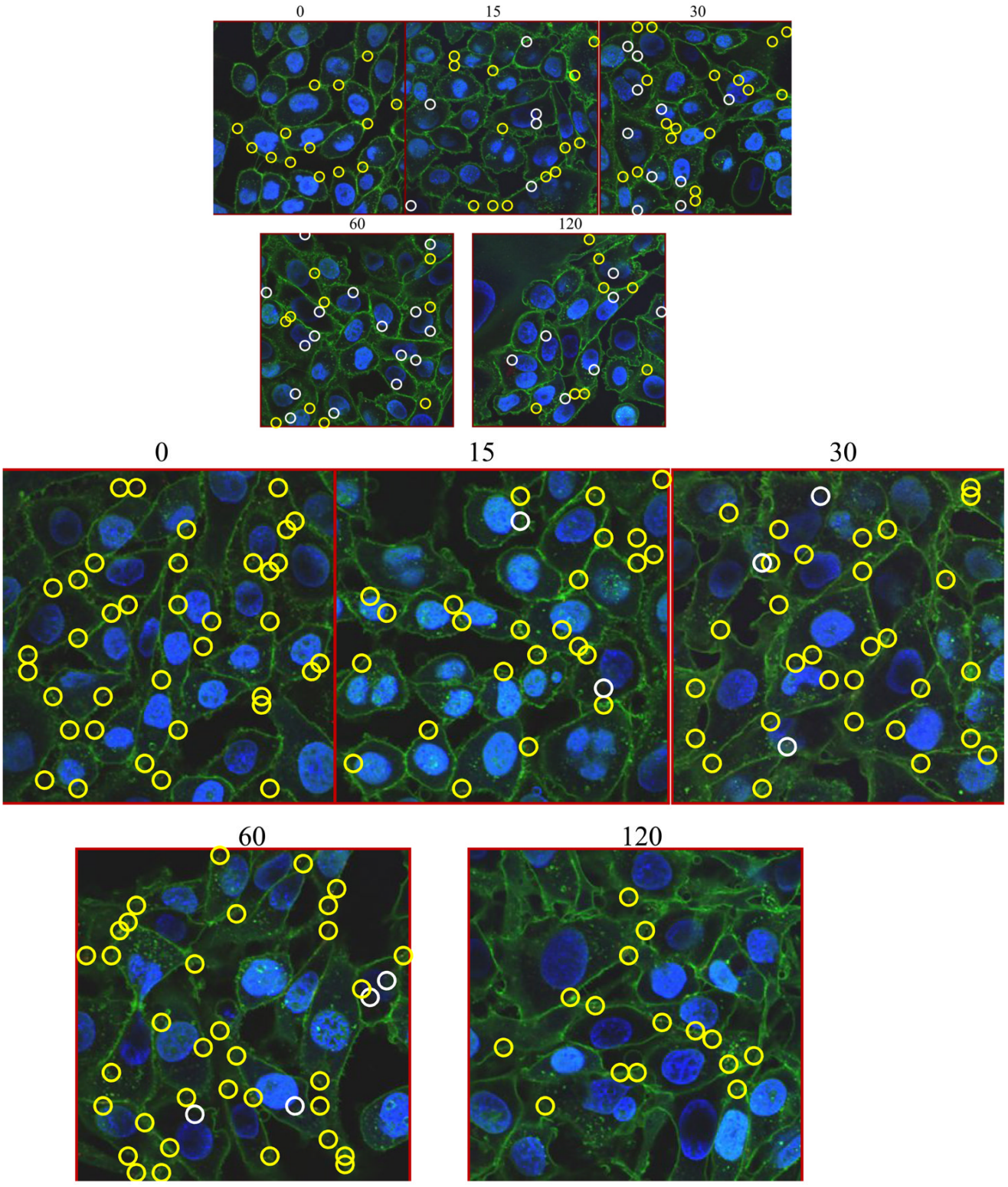

Fig. 8.

(A) CHO-K1 cells were mock treated (top panels) or (B) treated with 100 μM Y-27632 for 30 min at 37°C. Cells were chilled on ice for 10 min and then L11VP26mRed (MOI 10) was

incubated on the cells at 4°C for 2 h in the absence (A) or presence (B) of Y-27632 (100 μM). 37°C media with or without Y-27632 was added to the cells and then the cells were fixed and stained at 0, 15, 30, 60, and 120 min. with Hoechst and wheat germ agglutinin to label the nucleus (blue) and plasma membrane (green), respectively. Capsids (red) were observed with a confocal microscope. Nuclear-associated capsids are circled in white and non-nuclear associated capsids are circled in yellow.